

Loss Minimization Control of an Induction Motor Drive

Parviz Famouri and Jimmie J. Cathey, *Senior Member, IEEE*

Abstract—This paper presents a practical method for operation of an inverter-fed induction motor drive at the point of maximum efficiency while maintaining any particular torque-speed load point. Design and operation of an economical, microprocessor-based adaptive controller used to modify a commercially available six-step inverter for minimum loss operation of an induction motor is described. Experimental results are presented in graphical form, giving comparison of overall drive system efficiencies between loss minimization control and constant volts/hertz control operation for a standard-efficiency induction motor with a 10-hp rating. The greatest potential for energy savings is found to exist for the case of loads with nonlinear torque-speed characteristics, such as a fan or pump load.

NOMENCLATURE

f	frequency of primary currents
f_r	frequency of secondary currents
I_1	primary current
I_2	secondary current (reflected)
N_m	shaft speed
$N_{\eta \max}$	speed at maximum efficiency
p	number of poles
P_1	total primary copper losses
P_c	total core losses
P_g	total average power across airgap
P_R	rotational losses
R_1	primary resistance
R_2	secondary resistance (reflected)
R_{ms}	core loss resistor
s	slip
T_e	total developed torque
T_L	load torque
X_1	primary leakage reactance
X_2	secondary leakage reactance (reflected)
X_{ms}	magnetizing reactance
η	efficiency
ω_m	shaft speed
ω_s	synchronous speed

INTRODUCTION

THERE ARE presently two classifications of commercially available inverter-fed adjustable-speed induction motor drives:

- 1) **Open loop:** The frequency is set to give approximately a desired speed while a constant volts/hertz ratio is maintained.

Paper IPCSD 90-17, approved by the Electric Machines Committee of the IEEE Industry Applications Society for presentation at the 1989 Industry Applications Society Annual Meeting, San Diego, CA, October 1–5. Manuscript released for publication June 16, 1990. This work was supported by Contract TCRD01-87-6011 from the Tennessee Center for Research and Development through the Power Electronics Applications Center, Knoxville, TN.

The authors are with the Department of Electrical Engineering, University of Kentucky, Lexington, KY 40506.

IEEE Log Number 9040509.

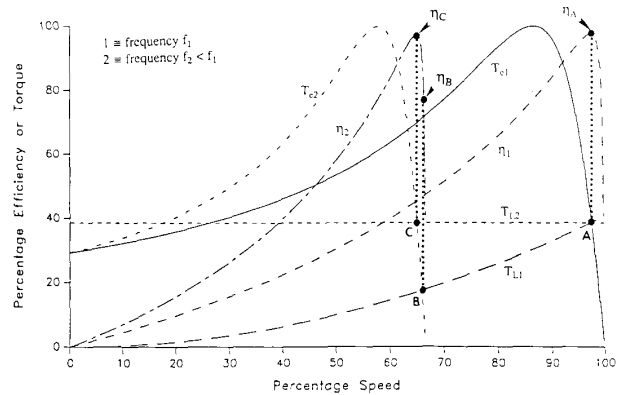


Fig. 1. Torque and efficiency characteristics.

- 2) **Closed-loop:** The speed loop is closed and speed feedback is also used to calculate a stator frequency command assuring that rotor frequency is held to a constant value (usually the value at rated or base operation) subject to the constraint that a volts/hertz ratio is not violated.

The open-loop inverter-fed drives offer the lowest initial cost and consequently dominate the industrial and commercial application population. At any particular control (frequency) setting, the open-loop inverter presents an available torque-speed curve; the curves labeled T_{e1} and T_{e2} of Fig. 1 exemplify control setting for two frequencies f_1 and f_2 . The point of operation is determined by the intersection of the load torque-speed characteristic with the available motor torque-speed curve. The typical efficiency-speed curves of Fig. 1 are used to illustrate that at some point A , the efficiency may have a maximum value η_A , whereas at some other control setting, where the simultaneous satisfaction of the motor and load torque curves is given by point B , it is observed that the efficiency η_B is a lower value than when operating at point A . It is seen that operation at maximum efficiency only occurs when the load and motor torque-speed characteristics intersect at the speed corresponding to the inflection point of the efficiency-speed curve $N_{\eta \max}$. Operation at maximum efficiency frequently takes place at near rated load torque; other load conditions result in reduced efficiency operation.

Temperature variation also has a significant effect on motor efficiency. As the temperature of the rotor increases, R_2 increases in value, the slope of the torque-speed curve decreases, and the operating point shifts such that it results in a lower value of efficiency.

The closed-loop inverter-fed drives can take advantage of the speed feedback signal for use in control of the inverter frequency f to assure a constant rotor frequency f_r according to the

algorithm

$$f = f_r + \frac{p}{120} N_m. \quad (1)$$

The rotor frequency chosen by set-up procedure is normally the value at rated or base speed, voltage, and frequency. If this value of rated rotor frequency results in near maximum efficiency, this closed-loop, constant rotor frequency (CRF) inverter can offer a small efficiency improvement over the popular open-loop constant volts/hertz (V/Hz) inverter. Although it potentially offers an efficiency improvement, the rotor frequency that yields maximum efficiency operation depends on parameters of the induction motor equivalent circuit, which can vary with temperature or saturation. Further, the value of rotor frequency that yields maximum efficiency performance is a function of motor speed. Thus, with no provision to adjust rotor frequency as either motor parameters or speed change, operation usually occurs at less than maximum efficiency.

During the past few years, several papers have appeared in the literature offering control regimes that attempt to maintain operation of adjustable speed drives at the maximum efficiency [1]–[5]. The potential for energy savings is significant, as is documented by [4] and [5]. However, all of these proposed control schemes require an accurate knowledge of the motor parameters for implementation. Maximum efficiency slip is more sensitive to the value of rotor resistance than any other motor parameter, yet rotor resistance changes with load profile, and dynamic measurement of its value is quite difficult, if at all possible.

Kusko and Galler [2] have offered mention of a testing controller concept that can be utilized to vary rotor slip frequency in a manner that minimizes input power while maintaining a particular torque-speed load point. Kirschen *et al.* [6] describe implementation of a testing or perturbing controller for minimum loss operation of a field-oriented controlled induction motor. Significant energy savings are found for operation at light torque loads for all speeds. For torque loads near nameplate rated value, energy savings at low-speed operation are reported.

In a recent thesis, Mehanna [7] presents an adaptive controller modification of a constant rotor frequency inverter to operate at optimal efficiency. The concept is similar to that used by Kirschen *et al.* [6], except that the extra complexity of the field-oriented control is not required. Further, since the adaptive controller can be realized by modification of a constant V/Hz inverter, it offers the potential of retrofit to inverters already in field service. The initial results of a computer simulation of this model are promising in that the controller has been demonstrated to be capable of seeking out the maximum efficiency slip point. Obviously, the advantage of this (perturbing rotor frequency (PRF)) scheme is that no knowledge of motor parameters is necessary; thus, parameter variations with temperature and saturation are of no consequence. Implementation and test of this concept are the subject of this paper.

THEORETICAL INVESTIGATION

A. Efficiency Determination

It is observed from Fig. 1 that for operation at any particular frequency, a pronounced inflection of the efficiency-speed curve of an induction motor exists. The Steinmetz equivalent circuit for the induction motor shown by Fig. 2 can be modified to account for frequency effects on copper and core losses as

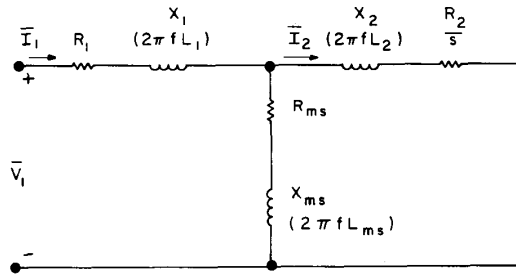


Fig. 2. Per phase equivalent circuit.

follows [8]:

$$R_1 = R_{10} + c_1 f \quad (2)$$

$$R_2 = R_{20} + c_2 (sf)^\alpha \quad (3)$$

$$R_{ms} = c_m f^\beta \quad (4)$$

where R_{10} and R_{20} are the dc values of R_1 and R_2 , respectively. Constants c_1 , c_2 , c_m , α , and β are determined from equivalent circuit parameters evaluated at two or more frequencies.

Let

$$R_{2m} + jX_{2m} = (R_{ms} + jX_{ms}) \parallel (R_2/s + jX_2) \quad (5)$$

and

$$\Delta = (R_{ms} + R_2/s)^2 + (X_{ms} + X_2)^2. \quad (6)$$

Then, the primary copper losses P_1 , the core losses P_c , and the power crossing the motor airgap P_g are given, respectively, as follows:

$$P_1 = \frac{3V_1^2 R_1}{(R_1 + R_{2m})^2 + (X_1 + X_{2m})^2} \quad (7)$$

$$P_c = \frac{3[(R_2/s)^2 + X_2^2] V_1^2 R_{ms}}{\Delta [(R_1 + R_{2m})^2 + (X_1 + X_{2m})^2]} \quad (8)$$

$$P_g = \frac{3(R_{2m}^2 + X_{2m}^2) V_1^2 R_2/s}{\Delta [(R_1 + R_{2m})^2 + (X_1 + X_{2m})^2]}. \quad (9)$$

As a reasonable approximation, the rotational power losses P_R are dependent on the square of speed, or

$$P_R = k_N \omega_m^2. \quad (10)$$

Since

$$\omega_m = (1-s)\omega_s = (1-s) \frac{2}{p} \omega = \frac{(1-s)4\pi f}{p} \quad (11)$$

(10) can be expressed for a four-pole motor as

$$P_R = k_N [\pi(1-s)f]^2. \quad (12)$$

Recalling that the power converted from electrical to mechanical form is given by $(1-s)P_g$, the per-unit efficiency of the induction motor is formed as a function of s , f , and V_1 :

$$\eta = f_1(s, f, V_1) = \frac{(1-s)P_g - P_R}{P_g + P_1 + P_c} \quad (13)$$

where P_1 , P_c , P_g , and P_R are square by (7)–(10), respectively. However, V_1 depends on the load torque T_L . Specifically, the developed electromechanical torque T_e must equal the sum of load torque and of torque due to rotational losses, or

$$T_e = \frac{(1-s)P_g}{\omega_m} = T_L + P_R/\omega_m. \quad (14)$$

Substitution of (9)–(11) into (14) and rearrangement leads to

$$V_1 = \left[\frac{s\pi f \Delta [(R_1 + R_{2m})^2 + (X_1 + X_{2m})^2] [T_L + k_N(1-s)\pi f]}{3R_2(R_{ms}^2 + X_{ms}^2)} \right]^{1/2}. \quad (15)$$

In general, $T_L = T_L(\omega_m)$ is speed dependent; thus, substitution of (15) into (13) yields efficiency as a function of s , f , and ω_m :

$$\eta = f_2(s, f, \omega_m) = \frac{f_3(s, f, \omega_m) - f_4(s, f)}{f_5(s, f, \omega_m)} \quad (16)$$

where

$$f_3 = \pi s(1-s)fR_2(R_{ms}^2 + X_{ms}^2)[T_L + k_N\pi(1-s)f] \quad (17)$$

$$f_4 = k_NsR_2[(1-s)f]^2(R_{ms}^2 + X_{ms}^2) \quad (18)$$

$$\begin{aligned} f_5 = & [T_L + k_N\pi(1-s)f]\{sR_2(R_{ms}^2 + X_{ms}^2) \\ & + R_1[(sR_{ms} + R_2)^2 + s^2(X_2 + X_m)^2] \\ & + R_{ms}[R_2^2 + s^2X_2^2]\}. \end{aligned} \quad (19)$$

In principle, each occurrence of s in (16) could be replaced by $s = (\pi f - \omega_m)/\pi f$ (four-pole case) to find $\eta = f_6(f, \omega_m)$. Then, for any particular value of ω_m , the value of $f = f_{\eta \max}$ that satisfies $\partial\eta/\partial f = 0$ is the value of frequency to yield maximum efficiency operation. However, the resulting expressions do not allow closed-form solution for $f = f_{\eta \max}$. Since a numerical solution for $f_{\eta \max}$ is inevitable, an alternate limited-range search approach is utilized in that $s = (\pi f - \omega_m)/\pi f$ is substituted into (16), and with ω_m held constant, η is evaluated as f is varied by small increments until $f = f_{\eta \max}$ is determined.

B. Theoretical Predictions

The plots of Fig. 1 are calculated using manufacturer supplied typical rated frequency and voltage values of equivalent circuit constants (see Appendix) for the standard-efficiency induction motor under test. Study of curves of Fig. 1 allows important observations concerning the efficiency comparison of PRF and V/Hz control. First, consider that the two load torque characteristics $T_{L1}(=k_1N_m^2)$ and $T_{L2}(=k_2)$ both result in maximum efficiency operation at point A . If the motor frequency is reduced so that the motor is characterized by curve 2, the constant torque load T_{L2} results in operation at point C , where efficiency η_c remains near maximum possible value. However, if the motor load torque is described by T_{L1} , operation at point B results with associated efficiency η_B , which is less than the maximum possible value. If the control regime is constant V/Hz, operation must remain with efficiency η_B . On the other hand, if PRF control is used, the perturbing controller will increase frequency and reduce voltage so that speed is unchanged while operation occurs at the maximum efficiency point

of a new curve slightly to the right of curve 2. Hence, it is predicted that PRF control offers efficiency improvement when the driven mechanical load presents a nonlinear torque-speed characteristic.

Second, if the constant load torque curve T_{L2} of Fig. 1 were reduced in magnitude, points A and C would move to the right along T_{e1} and T_{e2} , respectively, to yield operation at less than maximum efficiency. PRF control can allow adjustment of voltage and frequency to restore maximum efficiency operation.

Thus, efficiency improvement is expected when using PRF control for the case of reduced value constant load torque.

In order to substantiate the above predictions, two computer programs were built up to model the motor performance for both PRF and constant V/Hz operation. For both programs, the motor was modeled by the approximate frequency-dependent parameters documented in the Appendix and selected by guidance from [8]. The motor load torque was characterized as dependent on speed squared with value equal to the rated value at 100% motor speed. The first program predicted PRF performance using the limited-range search approach described in the previous section.

The second program calculated constant V/Hz performance with V_1/f maintained at the value determined by ratio of nameplate rated values. Implementation was carried out by substituting $V_1 = f(V_1/f)_{\text{rated}}$ and $f = \omega_m/(1-s)\pi$ into (14) and incrementing s from a small value until the equality of (14) was established.

Results of the theoretical study are presented by Figs. 3–5. Fig. 3 shows that for speed less than approximately 65% with the squared-law torque load, significant efficiency improvement is shown by PRF control over constant V/Hz control. Figs. 4 and 5 illustrate that for the lower speed operation, the PRF control acts to lower voltage and increase frequency over constant V/Hz control at each operating point to result in a reduction in core losses and, subsequently, to reduce the total losses.

EXPERIMENTAL INVESTIGATION

A. Controller Realization

In order to verify the theoretical predictions, an adaptive controller is built up by modification of a commercially available, six-step, 15-kVA, constant V/Hz inverter. An optional control card offered by the inverter manufacturer is installed in the inverter. The card provides the normal inverter adjustments for setting acceleration, deceleration, and V/Hz ratio. However, two features of the card are of particular interest in the design of the controller that is the focus of the described research. First, the slip signal input can be a bidirectional signal to dynamically alter the V/Hz control ratio, allowing control of the dc link voltage of the inverter independent of inverter output frequency. Second, the card accepts a square-wave input reference signal to directly control the inverter output frequency. In-house circuit designs are implemented to allow operation in either of two modes: 1) constant rotor frequency control, in which external command of rotor frequency is set and the controller acts to adjust dc link voltage magnitude to maintain the set speed and 2) perturbing control, in which rotor frequency command is per-

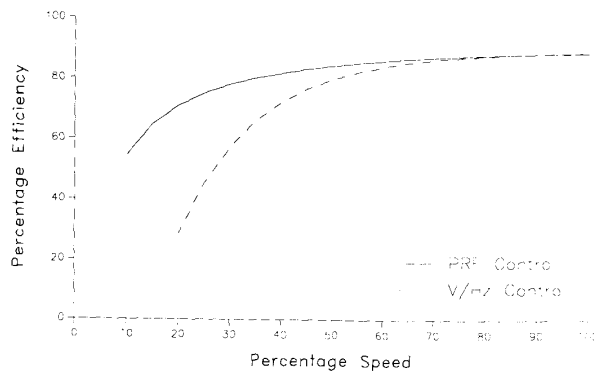


Fig. 3. Efficiency-speed characteristics.

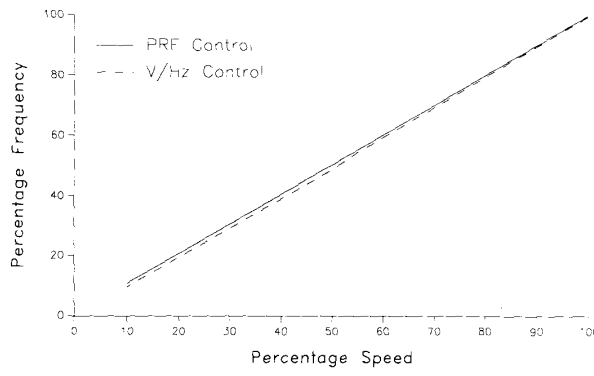


Fig. 4. Frequency-speed characteristics.

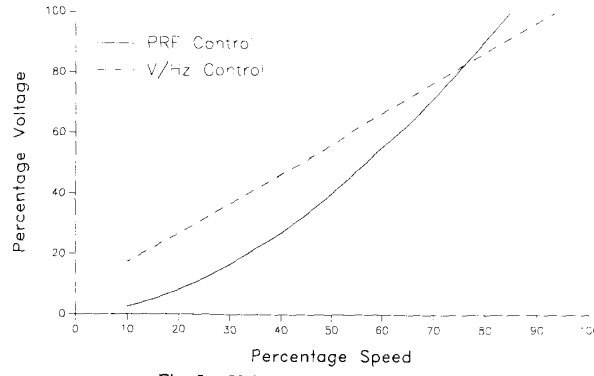


Fig. 5. Voltage-speed characteristics.

turbed in a manner to search for minimum input power while dc link voltage is adjusted to maintain the set speed.

A block diagram of the adaptive perturbing controller is presented in Fig. 6. Speed command Ω_m and actual motor speed ω_m are compared by the speed summer to yield the speed error signal v_E . v_E is processed by the PI controller to give the error signal v'_E used to set the value of bias signal Δv_{dc} that adjusts the V/Hz ratio, thus changing the dc link voltage. If ω_m is greater than Ω_m , the dc link voltage is reduced. Conversely, if Ω_m exceeds ω_m in value, the dc link voltage is increased, and thus, speed is regulated.

The inverter frequency command ω is formed by the frequency summer as a linear combination of the speed command

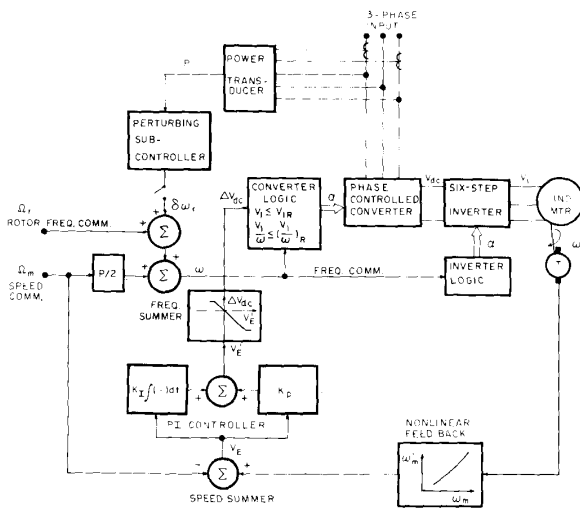


Fig. 6. Block diagram of adaptive controller.

Ω_m and the set rotor frequency command Ω_r . If the perturbing subcontroller is active, rotor frequency command Ω_r is altered by signal $\delta\omega_r$.

The perturbing subcontroller senses the inverter input power P and then either increases or decreases signal $\delta\omega_r$. If a change in $\delta\omega_r$ reduces the value of P , the perturbing subcontroller then changes $\delta\omega_r$ another increment in the previous direction. If inverter power P increases due to a change in $\delta\omega_r$, then the subcontroller begins to alter $\delta\omega_r$ in the opposite direction. Hence, the inverter output frequency is adjusted until a point at which minimum input power to maintain the mechanical load point is reached.

Although the controller concept has been presented by analog block diagram, the actual realization is better suited to a digital implementation. An 8-b microprocessor-based implementation of the controller is used. Introduction of 12-b A/D and D/A converters is necessary to obtain the performance accuracy required by the problem. An abbreviated flowchart of the adaptive controller program is displayed in Fig. 7 to give an understanding of the controller logic.

B. Test Descriptions

Losses of components under test are measured by the principle of air calorimetry to circumvent the error that can be introduced by electrical instruments with inadequate frequency response. The calorimetric loss determination technique was used to measure converter (cascaded ac-dc converter and inverter) losses P_{cL} and motor losses P_{mL} according to the test setup indicated by Fig. 8. A thorough presentation of the air calorimetry loss determination procedure is made in [9].

Two power conditioner-motor arrangements were tested: 1) standard-efficiency motor fed by six-step inverter using constant V/Hz control and 2) standard-efficiency motor fed by six-step inverter using perturbing rotor frequency control. Tests were conducted for motor speed ω_m of 25, 50, 75, and 100% of 1750 r/min. At each speed point, mechanical load was adjusted to require a shaft torque of 1/4, 2/4, 3/4, and 4/4 of 30 ft · lb, all under a thermal steady-state condition. In addition, data were recorded for both power conditioner-motor arrangements at 75% speed with 9/16 of 30 ft · lb. Thus, data were recorded for a

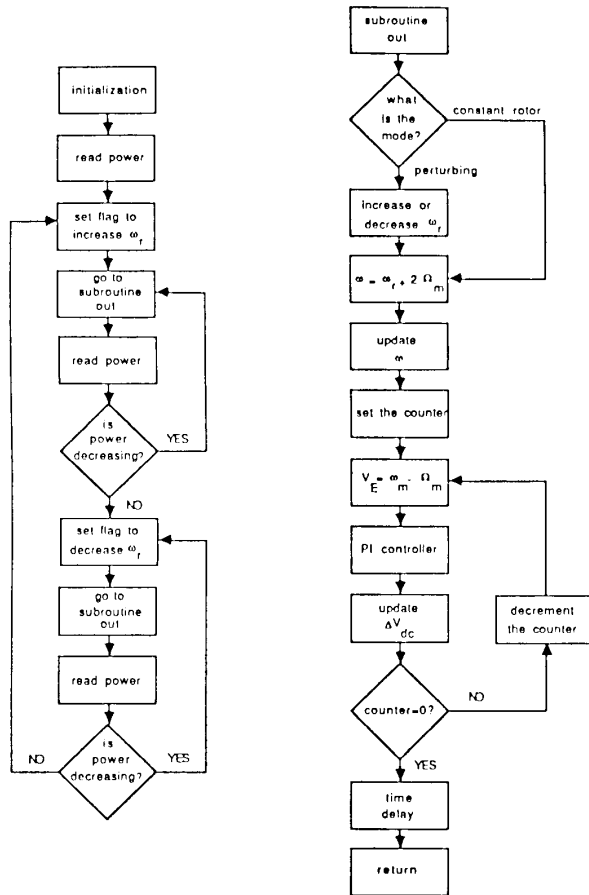


Fig. 7. Flowchart of controller program.

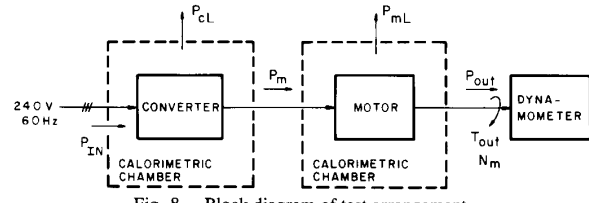


Fig. 8. Block diagram of test arrangement.

total of 17 torque-speed points for each of the two power conditioner-motor arrangements.

RESULTS OF TESTS

Data were recorded according to the description of the test set forth in the previous section. Fig. 9 displays photographs of recorded traces of input power and rotor frequency command for the case of 50% speed-1/4 torque, illustrating the dynamic nature of the PRF control. The rotor frequency has decreased by 23 steps for 0.05 Hz/step from 1.33 Hz to 0.19 Hz; meanwhile, input power has decreased by 2.75% for standard-efficiency induction motor.

The PRF control is successful in finding an operation point to improve motor efficiency and, consequently, the overall system efficiency over the V/Hz control. Figs. 10 and 11 show percentage efficiency versus speed for 1/4 and 4/4 torque, respectively,

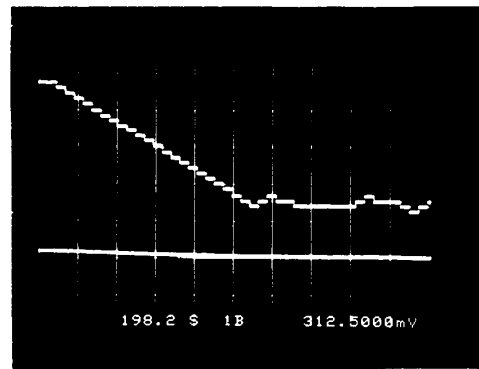


Fig. 9. Rotor frequency (upper trace) and input power (lower trace).

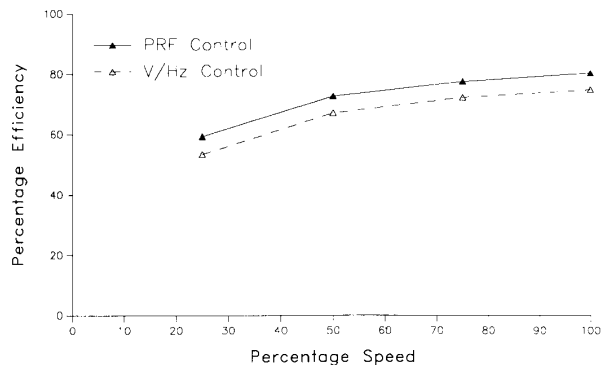


Fig. 10. Efficiency-speed data for 1/4 torque.

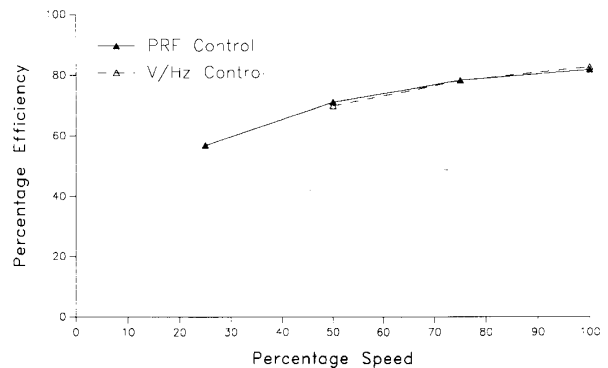


Fig. 11. Efficiency-speed data for 4/4 torque.

comparing overall system efficiency for V/Hz control and PRF control. As torque increases, the efficiency improvement of PRF over V/Hz decreases to an insignificant value, thus substantiating the earlier prediction that significant efficiency improvement only for reduced torque loads is to be expected.

The specific impact of the previous conclusion that the nonlinear torque load type is best suited for PRF control can be seen quantitatively from the plot of the square-law torque load data in Fig. 12. Then, the torque demand at 75 and 50% speed would be 56.25 (9/16) and 25% (1/4) of rated torque, respectively. The experimentally obtained efficiency at these points are 78.6 and 65.27%, respectively, using V/Hz control, whereas the efficiency would be improved by 1.4 and 7.46%, respectively, by use of PRF control.

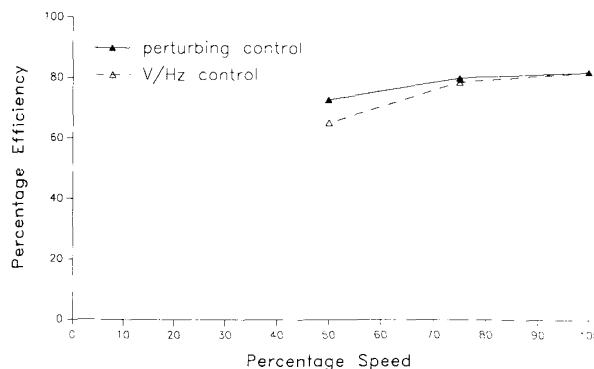


Fig. 12. Efficiency-speed data for square-law torque.

CONCLUSIONS

Comparison of test results leads to conclusions similar to those of [6] that reported work conducted with the more sophisticated field-oriented control:

- 1) Significant efficiency improvement over constant volts/hertz operation is offered by the loss minimization control at reduced torque loads for all speeds.
- 2) Small efficiency improvement is found for near rated torque loads at low-speed operation.

It is concluded that the greatest efficiency improvement is found for application of the loss minimization control when driving loads with nonlinear torque-speed characteristics, such as fan or pump loads. Such loads are already the primary application of constant volts/hertz inverter-fed induction motor drives. Further, since the described controller is suitable for economical retrofit of existing constant volts/hertz inverter drives, the practical interest should be significant.

APPENDIX

MACHINE PARAMETERS

Nameplate Data:

10 hp, 230/460 V, 27/13.5 A
1755 r/min 60 Hz, Design B
1.15 SF.

Equivalent Circuit Parameter (60 Hz):

$$\begin{aligned} R_1 &= 0.2264 \Omega & R_2 &= 0.1256 \Omega \\ X_1 &= 0.5842 \Omega & X_2 &= 0.7292 \Omega \\ R_{ms} &= 0.8382 \Omega & X_{ms} &= 10.367 \Omega \\ &\text{230-V connection.} \end{aligned}$$

Frequency-Dependent Model:

$$\begin{aligned} R_{10} &= 0.2151 \Omega & c_1 &= 0.8868 \times 10^{-4} \\ R_{20} &= 0.1231 \Omega & c_2 &= 1.236 \times 10^{-3} \\ c_m &= 2.2133 \times 10^{-3} & \alpha &= 1.75 \\ \beta &= 1.45 \end{aligned}$$

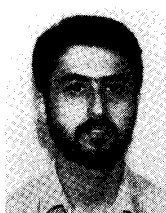
REFERENCES

- [1] D. Galler, "Energy efficient control of ac induction motor driven vehicles," in *Proc. 1980 IEEE-IAS Ann. Mtg.*, 1980, pp. 301-308.
- [2] A. Kusko and D. Galler, "Control means for minimization of losses in ac and dc motor drives," *IEEE Trans. Industry Applications*, vol. IA-19, no. 4, pp. 561-570, July-Aug. 1983.
- [3] M. H. Park and S. K. Sul, "Microprocessor-based optimal-efficiency drive of an induction motor," *IEEE Trans. Ind. Electron.*, vol. IE-31, no. 1, pp. 69-73, Feb. 1984.
- [4] J. M. D. Murphy and V. B. Honsinger, "Efficiency optimization of inverter-fed induction motor drives," in *Proc. 1982 IAS Ann. Mtg.*, 1982, pp. 544-552.
- [5] D. S. Kirschen, D. W. Novotny, and W. Suwanwisoot, "Minimizing induction motor losses by excitation control in variable frequency drives," *IEEE Trans. Industry Applications*, vol. IA-20, no. 5, pp. 1244-1250, Sept.-Oct. 1984.
- [6] D. S. Kirschen, D. W. Novotny, and T. A. Lipo, "Optimal efficiency control of an induction motor drive," *IEEE Trans. Electron. Comput.*, vol. EC-2, no. 1, pp. 70-76, Mar. 1987.
- [7] C. Y. Mehanna, "Perturbing controller for minimum loss operation of induction machines," M.S. thesis, Univ. Kentucky, Aug. 1985.
- [8] A. Bellini, R. Miglio, U. Reggiani, and C. Tassoni, "Voltage-frequency law in frequency-controlled induction motor drives," in *Proc. 1978 IEEE-IAS Ann. Mtg.*, 1978, pp. 690-693.
- [9] J. J. Cathey, M. Rabiee, and S. H. Jan, "Application of calorimetry in efficiency determination of power conditioned drives," *Electric Mach. Power Syst.*, vol. 14, no. 1, pp. 33-44, 1988.

Parviz Famouri was born in Tehran, Iran, on September 14, 1960. He received the B.S. degree in applied mathematics from Kentucky State University in 1981. He then began his studies at the University of Kentucky, where he received the B.S.E.E., M.S.E.E., and Ph.D. degrees in 1982, 1986, and 1990, respectively.

His research interest is in the control of electric machines.

His research interest is in the control of electric machines.



Jimmie J. Cathey (S'64-M'66-SM'83) was born in Whitney, TX, on May 16, 1941. He received the B.S.E.E. degree from Texas A&M University, the M.S.E.E. degree from Bradley University, and the Ph.D. degree from Texas A&M University in 1965, 1968, and 1972, respectively.

In 1965, he joined Caterpillar Tractor Company as a Research Engineer. For the periods 1968-1969 and 1972-1980, he was an employee of Marathon LeTourneau Company, progressively holding the positions of Project Engineer, Chief Electrical Engineer, and Director-Applied Research. Since 1980, he has been at the University of Kentucky, where he is presently a Professor of Electrical Engineering.

Dr. Cathey is a Registered Professional Engineer in the state of Texas and a member of Tau Beta Pi, Eta Kappa Nu, and Phi Kappa Phi.

